VERIZONA PUBLISHER
Publishing Your Ideas

www.verizonaonlinepublishing.com
Vol: 1, Issue: 1

Journal of Robotics and Mechanical Engineering Research

Stress Analysis of a Total Hip Replacement Subjected to Realistic Loading Conditions

Mohammad Rabbani and Hossein Saidpour*
School of Computing, Information Technology and Engineering, University of East London, UK

***Corresponding author:** Hossein Saidpour, School of Computing, Information Technology and Engineering, University of East London, UK; Email: S.H.Saidpour@uel.ac.uk

Article Type: Research, **Submission Date**: 13 April 2015, **Accepted Date:** 21 May 2015, **Published Date:** 11 June 2015.

Citation: Mohammad Rabbani and Hossein Saidpour (2015) Stress Analysis of a Total Hip Replacement Subjected to Realistic Loading Conditions. J Robot Mech Eng Resr 1(1): 18-23.

Abstract

In this paper the stress distribution of a complete assembly of femur and hip prosthesis is investigated with realistic boundary conditions under nine routine activities using finite element analysis. In each activity, different forces of varying magnitude and orientation were applied on the prosthesis during a period of time to examine the critical points developed in the entire 3D model. This includes a full description of the geometry, material properties and the boundary conditions. The activities considered comprise slow walking, normal walking, fast walking, upstairs, down stairs, standing up, sitting down, and standing on 2-1-2 legs and knee bending. The findings of this study can be used to develop more optimized hip joint prosthesis by altering the prosthesis geometry to achieve a more balanced stress distribution.

Keywords: Hip joint prosthesis, finite element analysis.

Introduction

The increase in ageing population has resulted in a sharp rise in the number of orthopaedic surgeries, which has changed from 130267 operations in 2006/7 to 178983 operations in 2010/11 [1].

Total hip replacement implants are fixed to femur in two ways, namely cemented or cementless. The later method was more commonly used until a few years ago, the implant is fixed to the bone with PMMA bone cement (polymethyl methacrylate). However due to the issues in using the cemented hip prosthesis, the preferred method is now cementless [1]. The cemented hip replacement has decreased considerably from 54% in 2005 to 36% in 2010. While during the same period cementless procedure has increased from 22% to 43% (Figure 1). The main disadvantage in using the cement substance the exothermic heat resulted during the processing chemical reaction can potentially harm the bone tissues. However in the cementless design the parts are press fitted in the prepared bone, where the bone is expected to grow in crevices of the implant. This type of hip joint replacement is expected to last longer and eliminates pain.

In this paper a cementless hip joint prosthesis design is used to investigate the stress distribution on the prosthesis- femur assembly under nine different loading conditions using ANSYS software, as a finite element analysis (FEA) package, which simulates the frequent activities of daily living.

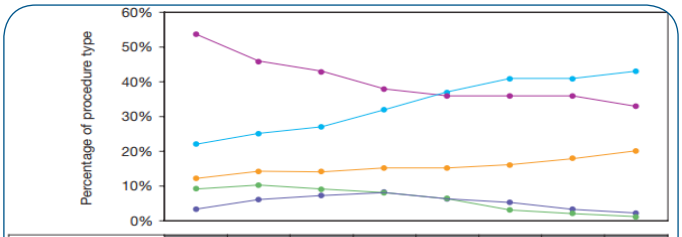

Year	2005	2006	2007	2008	2009	2010	2011	2012
Cemented	54%	46%	43%	38%	36%	36%	36%	33%
Cementless	22%	25%	27%	32%	37%	41%	41%	43%
Hybrid	12%	14%	14%	15%	15%	16%	18%	20%
Resurfacing	9%	10%	9%	8%	6%	3%	2%	1%
Large head metal-on-metal (≥36mm)	3%	6%	7%	8%	6%	5%	3%	2%
Number of procedures	56,454	59,967	67,321	70,559	70,908	73,006	75,460	76,448

Figure 1: Type of primary hip replacement procedures undertaken between 2005 and 2012 [1]

Boundary conditions

Many researchers have implemented different loading conditions on the hip joint prosthesis. They have used experimentally measured forces during gait and stairs climbing in extensive musculoskeletal studies [2-6]. Bergmann et al have presented a brief calculation of the mechanical loadings and the function of hip joint and proximal femur [2]. Their results indicate that the average person loaded their hip joint with a maximum of 238% BW (percent of body weight) when walking at about 4 km/h and with slightly less when standing on one leg. When climbing upstairs the joint contact force recorded 251% BW which is less than 260% BW when going downstairs. Inwards torsion of the implant is probably critical for the stem fixation. On average it was 23% larger when going upstairs than during normal level walking. The inter- and intra-individual variations during stair climbing were large and the highest torque values are 83% larger than during normal walking.

A typical coordinate system for measured hip contact forces is shown in Figure 2. The hip contact force vector $-F$ and its components $-F_x$, $-F_y$, $-F_z$ acts from the pelvis to the implant head and is measured in the femur coordinate system x, y, z. The magnitude of contact force is denoted as F. The axis z is taken as parallel to the idealized midline of the femur; x is parallel to the dorsal contour of the femoral condyles in the transverse plane.

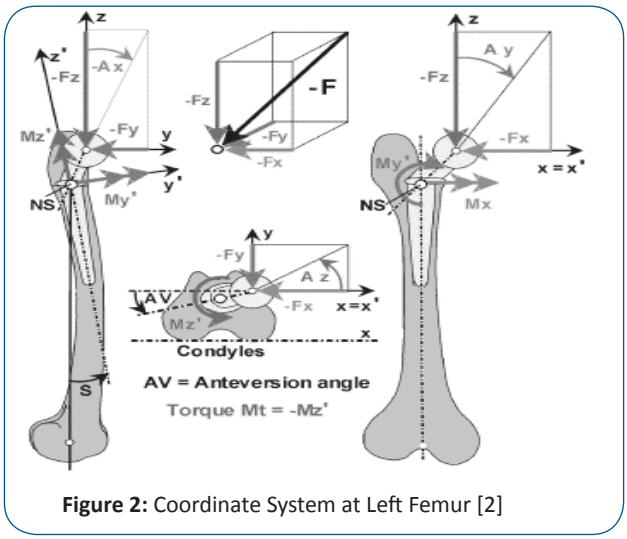

Figure 2: Coordinate System at Left Femur [2]

The contact force causes a moment M with the components M_x, $M_{y'}$ and $M_{z'}=-M_t$ at the point NS of the implant. A positive torsional moment M_t rotates the implant head inwards. M is calculated in the implant system x, y', z'. Both systems deviate by the angle S. AV is the anteversion angle of the implant [2]. One of the major factors to be considered is the loading condition. Some type of loads may have a more significant effect on the design. Biegler et al, [7] has developed a brief FE analysis and calculation of two designs of hip prostheses in one-legged stance and stair climbing configurations. They showed that the torsional loads during stair climbing contribute to larger amounts of implant micro motion than stance loading does.

The relative motion between the bone-prosthesis interfaces is more dependent on load type than on implant geometry or surface coating type. In addition, the resultant force of each activity is applied at a specific angle with respect to XY and XZ plane. There are various loading conditions tested on different patients. These real life activities are shown in different diagrams that include slow, normal and fast walking, upstairs, down stairs, standing up, sitting down and standing on 2-1-2 legs and also knee bending condition. Similar diagrams are introduced for moment M.

Apart from the resultant force applied on the prosthesis, there are few muscles attached to femur that induce extra tension on bone. At 85% of the gait cycle, a simplified set of active muscles are the abductor muscles, located on the greater trochanter (Gluteus medius and Gluteus minimus), and the ilio-tibial band (Gluteus maximus and tensor fascia latae) [8].

Furthermore Sowmianarayanan has worked on finite element analysis of proximal femur nail, and assumed the distal end of the femur model to be fully fixed [9]. According to Simoes et al, the various loads including body weight and different muscles at proximal femur were considered for this analysis [10].The applied loads consist of joint reaction force, abductor force, Iliopsoas force and vastas lateral and are close to data from El'Sheikh et al, [8]. In this study the relative forces and their location are listed and shown in Table1 and Figure 3.

In this study a series of 3D CAD models were produced in SolidWorks using a hip prosthesis manufactured by Johnson & Johnson. Then the resulted model was fitted into a 3D model of a femoral bone that is similar in shape and size to the

Table 1: Muscles-forces applied on the femur [8]

		Muscles		
		Gluteus Medius	Gluteus Minimus	Ilio-tibial band
Average Force (N)	F_x	-259	-279	-59
	F_y	160	269	-74
	F_z	319	134	-58

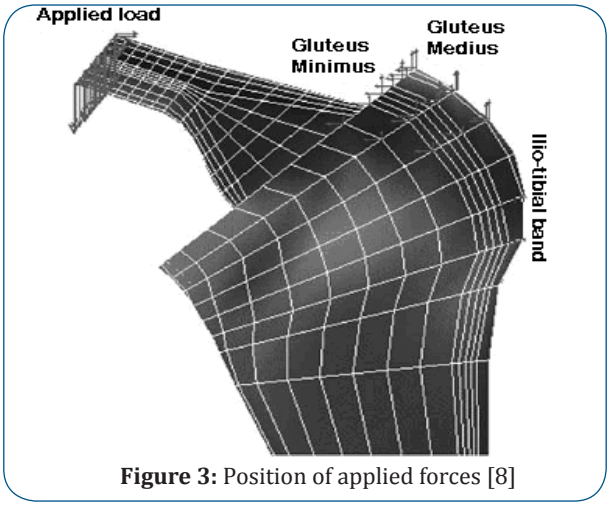

Figure 3: Position of applied forces [8]

standard femur. The 3D model of femur bone was created by 3D laser scanning in Redding Industries, Inc.

The Solid Works models of the prosthesis- femur assembly were subsequently imported to ANSYS for finite element analysis under 9 frequent activities of daily life including: slow walking, normal walking, fast walking, upstairs, down stairs, standing up, sitting down, and standing on 2-1-2 legs and knee bending. The relevant materials were assigned to different parts of the 3D model and then the whole assembly was meshed to achieve an overall 30341 nodes and 16095 elements. At each stage of the modelling process, different boundary conditions were applied for each of 9 activities during various time of action. This included all the relevant forces and moments.

The hip endoprosthesis examined was a cementless implant from J&J Company which consists of a femoral component and an acetabular component. The material assigned to the femoral stem was titanium. The material for acetabular cup and femoral head was considered to be Co-Cr and the plastic liner was ultra-high-molecular-weight polyethylene (UHMWPE). The femur bone has been assumed to be isotropic and linearly elastic. The relevant material properties have been taken from the findings of Bougherara et al, since the practical and theoretical results were found to be similar [11]. The bone properties assumed in this study include cortical (E = 10 GPa, υ = 0.3) and cancellous (E = 206 MPa, υ = 0.3) [11].

Data validation

Using ANSYS software it was possible to describe the stress in the same locations as those in which the strain gauges were applied in the practical experiment. The strain distributions are shown in Figure 5 for the neck and shaft of the synthetic femur. Strain values were taken for each individual strain gauge for each force that was applied in the practical experiment. The main strain

Table 2: The strain results of synthetic femur, subjected to various axial loading conditions, derived from FEA technique and measured by strain gauges at 6 femur locations as shown in Figure 5.

Applied Force (N)	Measuring method	Strain (με) values at 6 different points					
		1	2	3	4	5	6
305	Strain gauge	112	25	-165	-12	12	10
	FEA	108.6	23.9	-146.9	-10.7	11.3	7.2
594	Strain gauge	209	40	-329	30	10	6
	FEA	200.6	38.5	-306.8	-28.3	9.4	4.9
905	Strain gauge	322	70	-488	-32	14	18
	FEA	309.1	63.1	-453.4	-30.1	13.3	15.3
1210	Strain gauge	440	90	-655	-24	28	35
	FEA	422.4	86.2	-563.6	-21.6	25.8	29.6
1505	Strain gauge	565	123	-814	-19	-39	50
	FEA	536.8	116.9	-740.7	-17.8	-36.3	42.8

values are given in Table 2.

The comparison of FEA and strain gauge results are shown in Figure 4. This indicates that a very good correlation between the FEA and the experimental measurement of strain exists. Therefore it can be assumed that FEA is an accurate representation of how a body behaves when it undergoes an applied force. The application of FEA to improve a hip replacement has been found to be a viable method. In this study a 4th generation synthetic femur was used. This was made of a glass fibre polymer composite material and the properties were taken from the manufacturers handbook [12] and also confirmed with previous studies [13 -18]. Using this value it was possible to input the correct data into the ANSYS software for the simulation to be as accurate as possible.

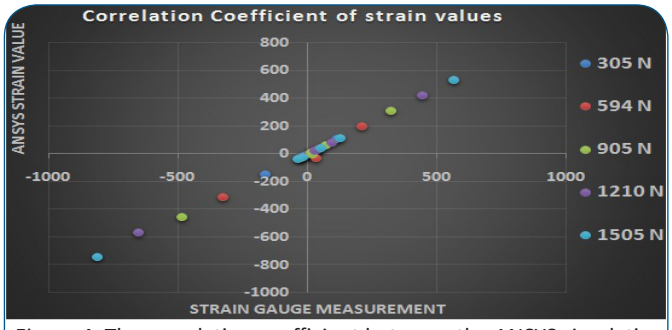

Figure 4: The correlation coefficient between the ANSYS simulation and the practical experiment results that shows a close value of R2=0.99

Results and Discussion

In this study three different stress distribution data including von Mises stress, maximum principal stress and shear stress have been assessed. The ANSYS generated output are shown in Figures 6. It should be noted that each of these nine activities was performed during different time intervals and ultimately the peak stress during each activity was evaluated to compare the performance of the prosthesis.

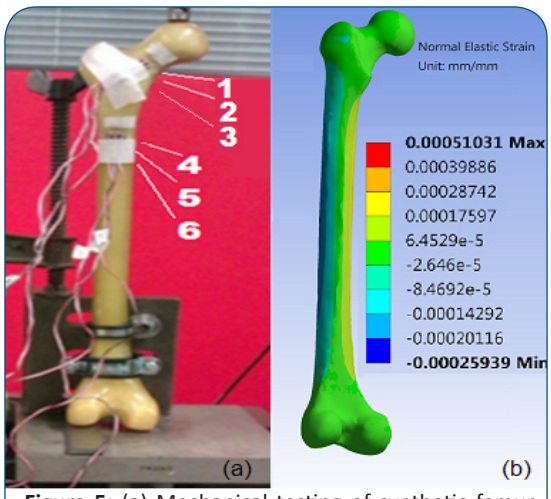

Figure 5: (a) Mechanical testing of synthetic femur, showing the locations of strain gauges used to measure strain. (b) Strain distributions in the synthetic femur

The results for fast walking indicate that von Mises stresses at the peak load shows the critical areas around the femoral neck and sharp edges of acetabular cup. Whilst the maximum principal stress distribution displays high tensile stresses on the upper side of the femoral neck (Figure 6). This is because the loads applied

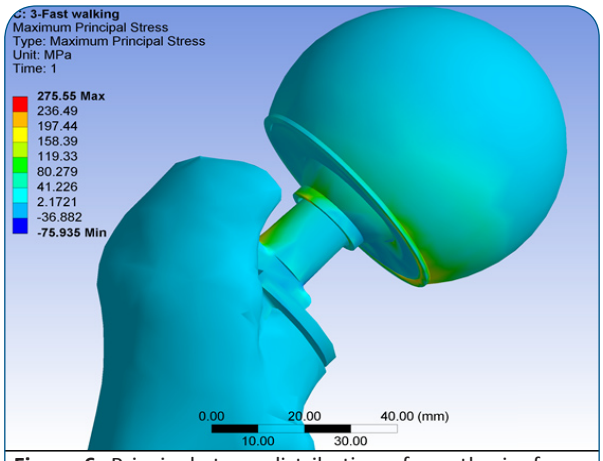

Figure 6: Principal stress distribution of prosthesis- femur assembly during fast walking at the time of peak load, showing high tensile stresses on the upper side of the femoral neck

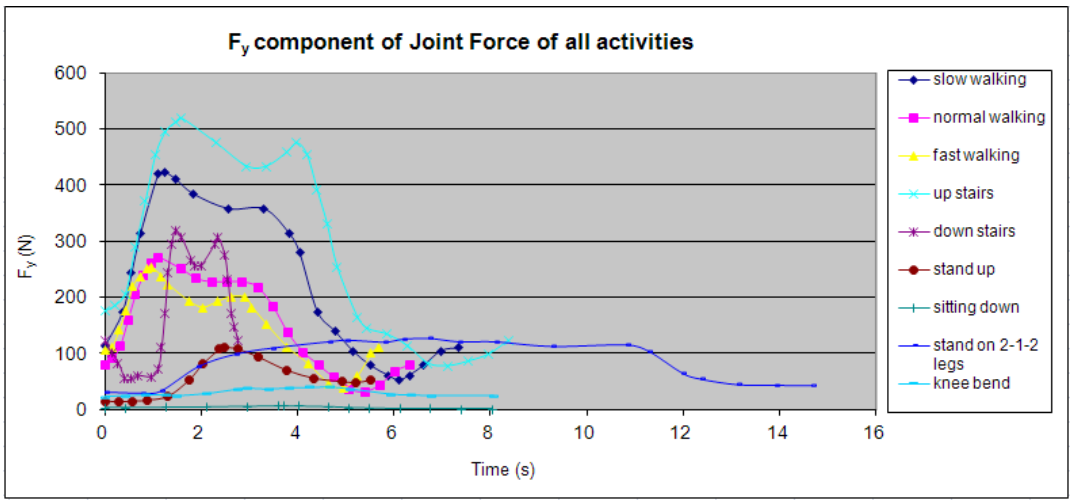

Figure 7: F_y component of joint force of all activities

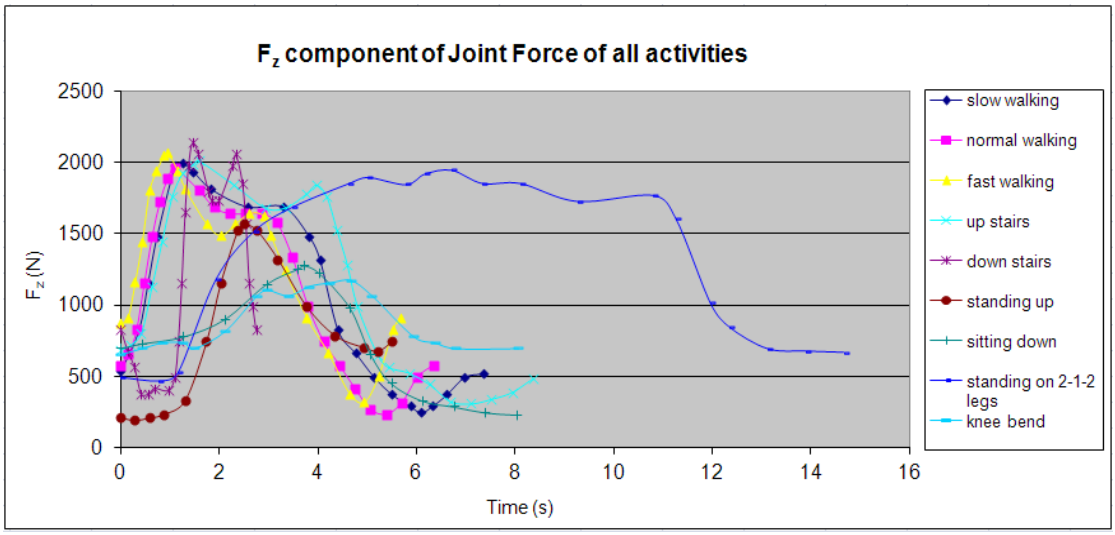

Figure 8: F_z component of joint force of all activities

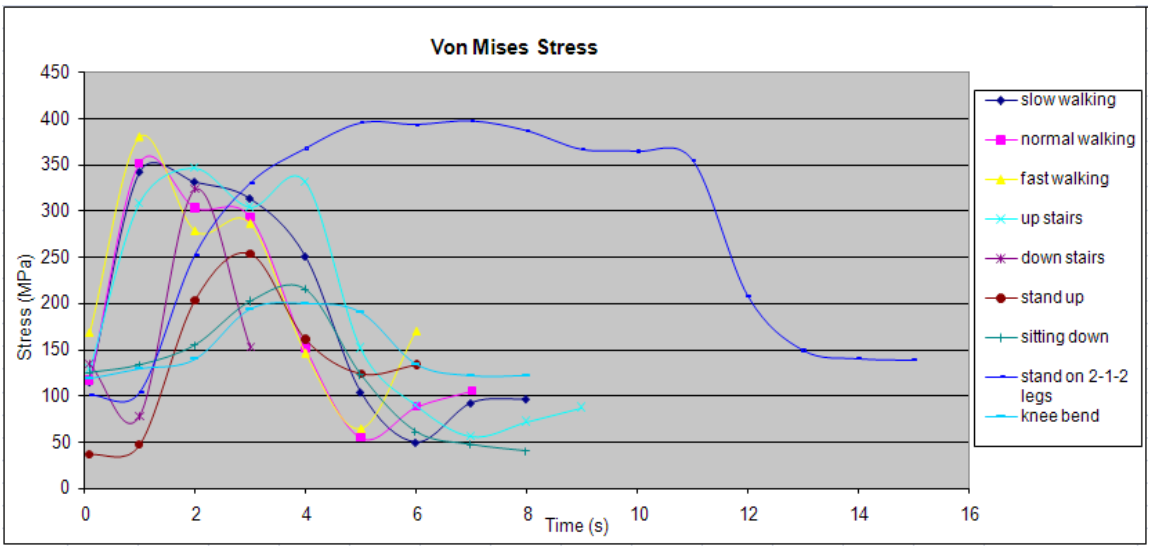

Figure 9: von Mises stress of nine activities during different time intervals

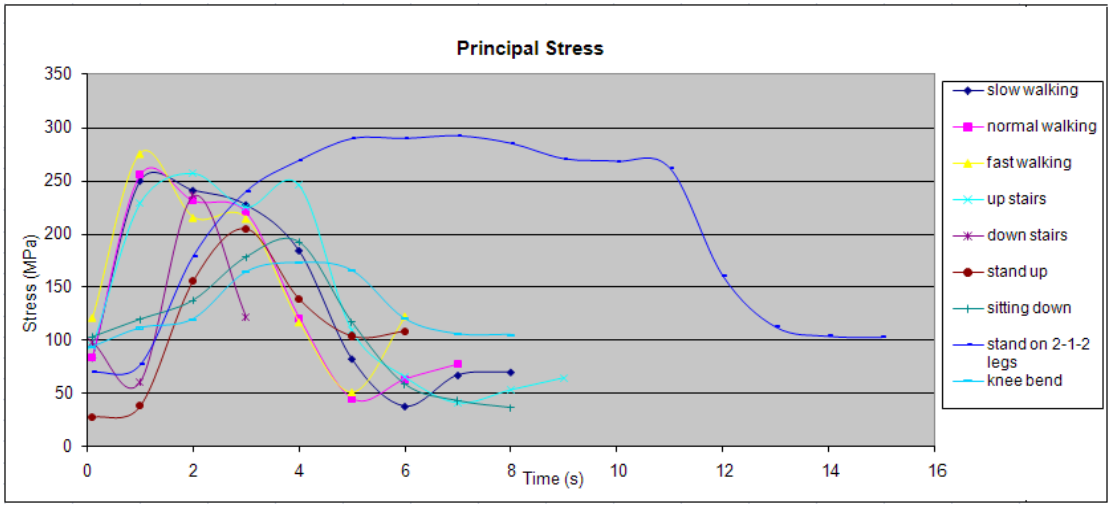

Figure 10: Principal stress of nine activities during different time intervals

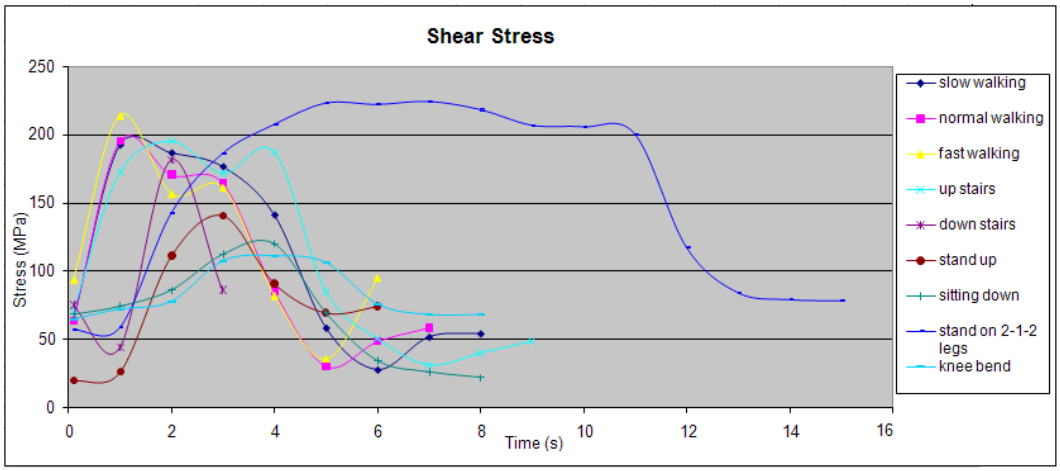

Figure 11: Shear stress of nine activities during different time intervals

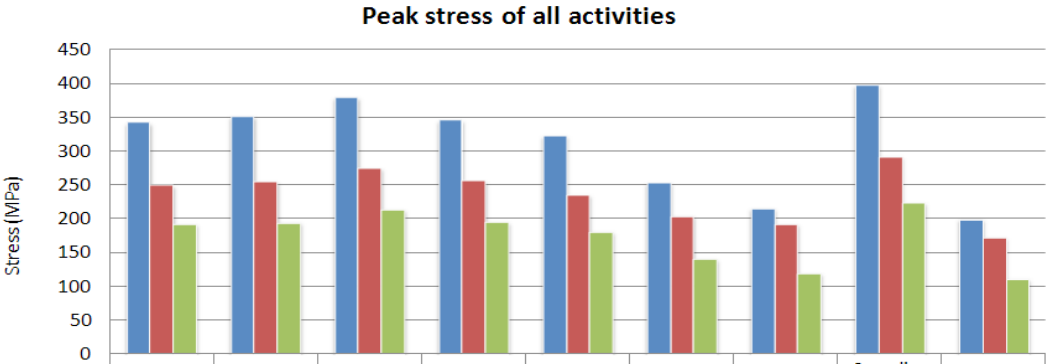

	Slow walking	Normal walking	Fast walking	Up stairs	Down stairs	Standing up	Sitting down	Standing on 2-1-2 legs	Knee bending
Max.Von Mises	342.45	351.93	379.94	345.95	323.48	253.67	215.97	398.05	199.97
Max.Principal	249.83	255.49	275.55	256.3	235.6	204.73	192.56	292.44	172.78
Max.Shear	192.48	195.01	213.82	195.36	181.42	140.99	119.95	224.05	111.44

Figure 12: Comparative study of peak stress of all activities

on the acetabular cup are eccentric and follows the specific angles. At the same time the shear stress distribution indicates the critical areas on the femoral cup.

The maximum von Mises stress during slow, normal and fast walking calculated as 342MPa, 352 MPa and 380MPa respectively. This shows throughout walking activity, stress increases gradually as speed of action rises. It indicates that going "upstairs" imposes more stress of about 23MPa on the joint than going "down stairs". This is similar situation with "standing up" and "sitting down". Although the last two actions apply considerably lower stress on the hip joint that going up or down stairs. The highest stress would be in "standing on 2-1-2 legs" activity by nearly 400MP in contrast with "bending knee" that enforces the lowest and only half of that stress on the joint by 200MPa (Figure 12). The stress

profile for von Mises stress, principal stress and shear stress shows lower values but follow almost the same curves (Figures 9-11). Also force patterns show that the component F_y which has a significant influence on the applied torque on the implant, is larger when going upstairs than all walking activities.

Down stairs the peak force slightly exceeds that from going upstairs. Standing up from a chair loads the hip join more than sitting down but much less than walking. The rotating component F_y is very small when sitting down (Figures 7 and 8).

Bergmann et al, [19] has also calculated the higher body weight percentage of about 409% of a patient with disrupted pattern which support the opinion that dysfunction of one muscle increases the joint contact force, because a part of the required joint moment is taken over by other muscles with unfavourably short lever arms and therefore higher forces.

Although proper inter-study comparison is difficult because of the variety of implant materials, implant geometries, and conditions used in the literature, resulting in a broad range of stress levels achieved on implant surfaces, however there are other studies presented on stress distribution of hip prosthesis. For example Mathias et al., has calculated the stress levels in the femoral component of a total hip prosthesis [20]. In that study they used a static point load of 2.5 KN that is applied vertically through the centre of the head of the femoral component. This load is approximately three times body weight, which is of the order of the load applied to the prosthesis in the living body. This study shows the status of a hip prosthesis under nine different loading conditions which can be effective to predict critical areas and important times of those activities so that we can optimise a design accordingly.

Conclusion

The purpose of this study was to investigate the biomechanical influence of different load type on the stress distribution through a hip implant. The critical areas were shown and discussed. The influence of speed and contribution of torsional load in different activities of living life was explained. These loading conditions have more influence than implant geometry or surface coating type. In this study the FEA was chosen, since it is a greatly validated technique [21]. The research data can be related to the application of Frost's law in bone remodelling in order to predict the bone growth in different areas.

References

1. NJR. 10th Annual Report. [Internet]. National Joint Registry for England and Wales. 2013 [Accessed on: 2013 Nov 10]; Available from: http://bit.ly/1yQCTL1.
2. Bergmann G, Deuretzbacher G, Heller M, Graichen F, Rohlmann A, Strauss J, et al. Hip contact forces and gait patterns from routine activities. J Biomech. 2001; 34(7):859–871.
3. Heller MO, Bergmann G, Deuretzbacher G, Durselen L, Pohl M, Claes L, et al. Musculo-skeletal loading conditions at the hip during walking and stair climbing. J Biomech. 2001; 34(7):883-893.
4. Lengsfeld M, Bassaly A, Boudriot U, Pressel T, Griss P. Size and Direction of Hip Joint Forces Associated With Various Positions of the Acetabulum. J Arthroplasty. 2000; 15(3):314-320.
5. Costigan PA, Deluzio KJ, Wyss UP. Knee and hip kinetics during normal stair climbing. Gait Posture. 2002; 16(1):31-37.
6. Stansfield BW, Nicol AC. Hip joint contact forces in normal subjects and subjects with total hip prostheses: walking and stair and ramp negotiation. Clin Biomech (Bristol, Avon). 2002; 17(2):130-139.
7. Biegler FB, Reuben JD, Harrigan TR, Hou FJ, Akin JE. Effect of porous coating and loading conditions on total hip femoral stem stability. J Arthroplasty. 1995;10(6):839-47.
8. El'Sheikh HF, MacDonald BJ, Hashmi MSJ. Finite element simulation of the hip joint during stumbling: a comparison between static and dynamic loading. Journal of Materials Processing Technology 2003; 143:249–255. doi: doi:10.1016/S0924-0136(03)00352-2.
9. Sowmianarayanan S, Chandrasekaran A, Krishnakumar R. Finite element analysis of proximal femur nail for subtrochanteric fractured femur. International ANSYS conference proceedings; 2006 [Accessed on: Aug 2013]; Available from: http://bit.ly/1wvmtSh.
10. Simo˜es JA, Vaz MA, Blatcher S, Taylor M. Influence of head constraint and muscle forces on the strain distribution within the intact femur. Med Eng Phys. 2000; 22(7):453–459.
11. Bougherara H, Zdero R, Shah S, Miric M, Papini M, Zalzal P, et al. Technical Note A biomechanical assessment of modular and monoblock revision hip implants using FE analysis and strain gage measurements. Journal of Orthopaedic Surgery and Research 2010; 5(34). doi:10.1186/1749-799X-5-34.
12. Sawbone 2014. [Accessed on: Feb 2014]. Available from: http://bit.ly/1GhCwwJ.
13. Chong ACM, Friis EA, Ballard GP, Czuwala PJ, Cooke FW. Fatigue performance of composite analogue femur constructs under high activity loading. Ann Biomed Eng. 2007; 35(7):1196-1205.
14. Chong ACM, Miller F, Buxton M, Friis EA. Fracture toughness and fatigue crack propagation rate of short fiber reinforced epoxy composites for analogue cortical bone. J Biomech Eng. 2007; 129(4):487-493.
15. Dunlap JT, Chong ACM, Lucas GL, Cooke FW. Structural properties of a novel design of composite analogue humeri models. Ann Biomed Eng. 2008; 36(11):1922-1926. doi: 10.1007/s10439-008-9568-y.
16. Heiner AD. Structural properties of fourth-generation composite femurs and tibias. J Biomech. 2008; 41(15):3282-3284. doi: 10.1016/j.jbiomech.2008.08.013.
17. Zdero R, Olsen M, Bougherara H, Schemitsch EH. Cancellous bone screw purchase: a comparison of synthetic femurs, human femurs and finite element analysis. Proc Inst Mech Eng H. 2008; 222(8):1175-1183.
18. Papini M, Zdero R, Schemitsch EH, Zalzal P. The biomechanics of human femurs in axial and torsional loading: comparison of finite element analysis, human cadaveric femurs and synthetic femurs. J Biomech Eng. 2007; 129(1):12-19.
19. Bergmann G, Graichen F, Rohlmann A. Hip joint forces during walking and running, measured in two patients. J Biomech. 1993; 26(8):969–990.
20. Mathias KJ, Leahy JC, Heaton A, Deans WF, Hukins DWL. Hip joint prosthesis design: effect of stem introducers. Med Eng Phys. 1998; 20(8):620–624.
21. Herrera A, Panisello JJ, Ibarz E, Cegoñino J, Puértolas JA, Gracia L. Long-term study of bone remodelling after femoral stem: a comparison between dexa and finite element simulation. J Biomech. 2007; 40(16):3615-25.